

Quasi-two-dimensional approach to states of an adsorbed atom

Milton W. Cole and Flavio Toigo*

*Department of Physics, The Pennsylvania State University,
University Park, Pennsylvania 16802*

(Received 20 October 1980)

A method is developed for solving the Schrödinger equation to obtain the eigenfunctions $\psi(z, \bar{R})$ and eigenvalues of an adsorbed atom. By solving a one-dimensional equation for a given position \bar{R} on the surface, one generates an effective potential $\epsilon(\bar{R})$ for the problem of lateral motion. The leading correction to this Born-Oppenheimer-like approach is expressed in analytic form. A numerical calculation for the case of He on graphite illustrates the simplicity and accuracy of the method. The mean distance of a ground-state ${}^4\text{He}$ atom is found to agree with an experimental result of Carneiro, Passell, Thomlinson, and Taub.

I. INTRODUCTION

With increasing attention being addressed to the problem of adsorbed films on homogeneous surfaces, theoretical approaches which offer both accuracy and computational simplicity become particularly appealing. The classic example is the popular two-dimensional (2D) approximation, which assumes that the adatom motion is confined strictly to a plane. While this method succeeds for some applications in achieving semiquantitative validity, it does not describe such features as lateral variation of the potential energy $V(\bar{r})$ and the attendant motion out of the plane. This paper presents a more realistic approach which, to lowest order, is not significantly more difficult computationally than the 2D approximation. Numerical calculations are presented for the specific case of individual He atoms on graphite, but the applicability is quite general.

We denote the particle coordinate normal to the surface as z and the lateral position as \bar{R} . For a given \bar{R} , the potential has a minimum value (V_{\min}) as a function of z at the position $z = \xi(\bar{R})$. We expect the ground-state wave function to be localized about this value, the extent depending on the mass m and the form of the potential. The motion along the surface will then follow the periodic variation of $\xi(\bar{R})$. This description motivates our choice of wave function,

$$\psi(\bar{R}, z) = g(z; \bar{R}) h(\bar{R}) \quad (1)$$

regarding g as a function of z , its form depending on \bar{R} . The analogy with the Born-Oppenheimer approach to treating diatomic molecules is evident. In both cases the solution of one part of the problem (here z motion) generates an effective potential for the other. The present calculation as a whole is facilitated if there is only small coupling between the parallel and perpendicular motions. This corresponds to relatively slow variation of the z -dependent form

of the potential over the surface. In general, there are correction terms, which we calculate in terms of gradients of $\xi(\bar{R})$ and the form of the potential. For the specific case of He on graphite, their magnitude is of order 1% of the binding energy. Even in this case the evaluation of this term is worthwhile because its inclusion brings the result into good agreement with experiment^{1,2} and a more conventional band-structure calculation.³

A method similar to ours has been proposed by Lai, Woo, and Wu.⁴ Our work differs in several respects, including the choice of the function g and by our having determined an explicit form for the correction term mentioned above.

The wave functions computed here may find use in a variety of applications. We illustrate this by determining the mean distance $\langle z \rangle$ of a ${}^4\text{He}$ atom from the top surface layer.

II. METHOD

We define a complete set of functions at each lateral position \bar{R} to be solutions of the 1D equation

$$\left[-\frac{\hbar^2}{2m} \frac{d^2}{dz^2} + V(z, \bar{R}) \right] g_n(z; \bar{R}) = E_n(\bar{R}) g_n(z; \bar{R}) \quad (2)$$

which are orthonormal with respect to z integration. Then a general solution of the Schrödinger equation can be written

$$\psi(z, \bar{R}) = \sum_n a_n(\bar{R}) g_n(z; \bar{R}) \quad (3)$$

Inserting this into the Schrödinger equation yields

$$\sum_n \left\{ a_n \left[-\frac{\hbar^2}{2m} \left(\frac{d^2}{dz^2} + \nabla^2 \right) + V(z, \bar{R}) - E \right] g_n - \frac{\hbar^2}{2m} (g_n \nabla^2 a_n - 2 \bar{\nabla} g_n \cdot \bar{\nabla} a_n) \right\} = 0 \quad (4)$$

Here the gradient refers to x and y coordinates. Multiplying by g_m^* and integrating over z yields

$$\left[E_m(R) - \frac{\hbar^2 \nabla^2}{2m} - \nabla_{mm}^2 - E \right] a_m - \sum_{n \neq m} (\nabla_{mn}^2 + \bar{A}_{mn} \cdot \bar{\nabla}) a_n = 0, \quad (5)$$

$$\nabla_{mn}^2 \equiv \frac{\hbar^2}{2m} \int dz g_n^* \nabla^2 g_n, \quad (6a)$$

$$A_{mn} \equiv (\hbar^2/m) \int dz g_m^* \bar{\nabla} g_n. \quad (6b)$$

Equations of the form (5) are coupled differential equations for the functions $a_m(\bar{R})$. Note that the coupling depends on the "off-diagonal" terms entering the summation. It is easy to show that they may be written

$$\left[\frac{m}{\hbar^2} \right] A_{mn} = [E_m(\bar{R}) - E_n(\bar{R})]^{-1} \int dz \bar{\nabla} g_m^* V(z; \bar{R}) g_n, \quad (6c)$$

$$\nabla_{mn}^2 = \sum_1 \bar{A}_{m1} \bar{A}_{1n} + \bar{\nabla} \cdot \bar{A}_{mn}. \quad (6d)$$

For the deeper bound states, these are small since they involve 2D gradients of the potential V divided by the energy separation of the g_n 's. In the numerical calculations described below, for example,

$$|\nabla_{01}^2| \sim 0.1 |\nabla_{00}^2| \leq 0.001 |E_0| m / \hbar^2.$$

In solving the coupled equations, their effect on the eigenvalues is proportional to the square of their magnitudes, divided by energy differences ($E_m - E_n$) between the diagonal terms. The resulting contributions to the eigenvalues E would be very small for widely spaced, deeply bound solutions of Eq. (2). Thus we neglect these for treating the lowest adsorption bands.

In this decoupling procedure, the function $h(\bar{R})$ of Eq. (1) becomes equal in turn to the various coefficients $a_m(\bar{R})$ in Eq. (3). From Eq. (5),

$$\left[-\frac{\hbar^2}{2m} \nabla^2 + \epsilon_m(\bar{R}) \right] h(\bar{R}) = E h(\bar{R}), \quad (7a)$$

$$\epsilon_m(\bar{R}) = E_m - \nabla_{mm}^2 \equiv E_m + \epsilon_c. \quad (7b)$$

The analogy with the Born-Oppenheimer procedure is apparent. Solving the z part of the problem for each \bar{R} generates the input $\epsilon_m(\bar{R})$ as an effective potential for the 2D wave function $h(\bar{R})$. The term ϵ_c represents an additional kinetic energy which would be absent from a naive procedure which assumed separability of the Schrödinger equation.

The present method offers several computational advantages over conventional band-structure calculations. One is that the principal \bar{R} variation of the wave functions is associated with the variation of $\xi(\bar{R})$, which may be treated explicitly. For the

ground-state band, one needs only the lowest ($m=0$) solution of Eq. (2). A conventional band-structure calculation, in contrast, requires a larger set of solutions of $V_0(z)$, the laterally averaged potential. Higher-lying states must be included there because they are admixed by the periodic potential and the concomitant variation of $\xi(\bar{R})$.

We note that the related problem of atomic beam scattering has been treated by a qualitatively similar technique—the corrugated hard wall method.⁵ By incorporating directly (via the $\psi=0$ boundary condition) a major aspect of the lateral variation, one simplifies thereby the ensuing calculation of scattering intensities.

Equation (2) can be solved either numerically or by fitting the z dependence of the potential to one of variety of analytic forms.⁶⁻⁹ Particularly convenient is the shifted-Morse potential,⁶

$$V_{SM}(z) = D \left\{ \exp\{-2\alpha[z - \xi(\bar{R})]\} - 2 \exp\{-\alpha[z - \xi(\bar{R})]\} - \Delta \right\}, \quad (8)$$

because its spectrum and eigenfunctions have analytic forms¹⁰

$$E_n = -D \left\{ \Delta + \left[1 - \left(\frac{2n+1}{b} \right) \right]^2 \right\}, \quad (9)$$

$$\phi_0 = [\alpha/\Gamma(b-1)]^{1/2} y^{(b-1)/2} e^{-y/2}, \quad (10a)$$

$$\phi_1 = (b-3)^{1/2} [1 - (b-2)/y] \phi_0, \quad (10b)$$

$$b = (8mD/\hbar^2 \alpha^2)^{1/2}, \quad (10c)$$

$$y = b \exp[-\alpha(z - \xi)]. \quad (10d)$$

Known potentials are well fitted in the vicinity of their minima [of depth $D(1+\Delta)$] by this form,^{6,7} and that is the important region for determining the strongly bound states. The incorrect form of V_{SM} at large z is irrelevant for these.⁶ With this parameterization, the energy shift ϵ_c associated with the ∇^2 term of Eq. (6) may be calculated. This analysis is presented in the Appendix, with an explicit expression given in Eq. (A1). Note that it is of second order in the gradients of α , b , and ξ . In the case discussed below, it is less than or of order 1% of the binding energy.

III. CALCULATIONS

We have tested this method by treating He isotopes on graphite, a case of particular experimental and theoretical interest. The input potential used is the anisotropic 6-12 potentials of Carlos and Cole.¹¹ It is consistent, within experimental error, with the 19 bound-state resonances and matrix elements obtained in scattering experiments by Derry *et al.*¹² and Boato *et al.*¹³

By fitting the z dependence of $V(z, \bar{R})$ to a

TABLE I. Parameters of the potential and ground-state energies (in meV) along symmetry lines of the basal-plane hexagon [see Eq. (14) for the notation].

$\vec{R} = (s_1, s_2)$	α (\AA^{-1})	D (meV)	Δ	ξ (\AA)	E_0	${}^3\text{He}$			${}^4\text{He}$			
						$\Delta\epsilon_p$	ϵ_c	$\epsilon(R)$	E_0	$\Delta\epsilon_p$	ϵ_c	$\epsilon(R)$
(0,0,0)	1.85	13.32	0.43	2.57	-14.07	0.06	0.0	-14.01	-14.67	0.04	0.0	-14.63
(0.1,0)	1.90	12.64	0.48	2.59	-13.64	0.07	0.13	-13.44	-14.24	0.05	0.12	-14.07
(0.2,0)	1.98	11.43	0.54	2.65	-12.75	0.09	0.19	-12.46	-13.32	0.06	0.17	-13.09
(0.3,0)	2.04	10.43	0.60	2.71	-11.91	0.11	0.11	-11.69	-12.46	0.07	0.10	-12.29
(0.4,0)	2.08	9.82	0.64	2.75	-11.38	0.13	0.03	-11.22	-11.91	0.08	0.03	-11.80
(0.5,0)	2.10	9.60	0.65	2.76	-11.20	0.13	0.0	-11.06	-11.73	0.09	0.0	-11.64
(0.05,0.05)	1.88	12.79	0.47	2.59	-13.74	0.06	0.11	-13.57	-14.34	0.05	0.09	-14.20
(0.1,0.1)	1.96	11.73	0.53	2.64	-13.00	0.08	0.20	-12.72	-13.57	0.06	0.17	-13.34
(0.15,0.15)	2.03	10.73	0.59	2.69	-12.20	0.11	0.17	-11.92	-12.76	0.07	0.16	-12.53
(0.2,0.2)	2.08	9.95	0.64	2.74	-11.56	0.13	0.09	-11.34	-12.10	0.08	0.08	-11.93
(0.25,0.25)	2.12	9.44	0.67	2.77	-11.13	0.14	0.03	-10.96	-11.66	0.09	0.02	-11.55
(0.3,0.3)	2.15	9.17	0.70	2.79	-10.92	0.15	0.01	-10.76	-11.44	0.09	0.0	-11.33
$(\frac{1}{3}, \frac{1}{3})$	2.15	9.14	0.70	2.79	-10.89	0.15	0.0	-10.73	-11.41	0.09	0.0	-11.32

shifted-Morse form, Eq. (8), one generates the values of D , α , ξ , and Δ at any \vec{R} . The arbitrary procedure we adopted for convenience was to set $V_{\text{SM}} = V(\vec{R}, z)$ at three points: $z = \xi(\vec{R})$ and $\xi(\vec{R}) \pm \delta z$. Denoting the values of V at these points by V_{min} and V_{\pm} , we obtain three equations. Defining $U = V - V_{\text{min}}$, the solutions are

$$\Delta = -(1 + V_{\text{min}}/D) , \quad (11a)$$

$$D = U_+ U_- (U_+^{1/2} - U_-^{1/2})^{-2} , \quad (11b)$$

$$\alpha = (1/\delta z) \ln[U_-/U_+]^{1/2} . \quad (11c)$$

Values of these parameters obtained with $\delta z = 0.3 \text{\AA}$ along symmetry axes are given in Table I. The points S , A , and SP denote the adsorption site, C atom position, and midpoint of the $C-C$ bond, respectively.¹⁴ We shall restrict our attention to the $n=0$ solutions in the following.

Although the potential V_{SM} fits $V(z, \vec{R})$ extremely well (to better than $\frac{1}{2}\%$) over a range 1\AA near the minimum, there is a non-negligible discrepancy at more distant points. Since the zero-point motion of these very light atoms extends somewhat farther out [$\sim (\hbar^2/mD)^{1/2}$ from ξ], a precise calculation requires computation of the effect of this error. From perturbation theory it is evaluated to be¹⁵

$$\Delta\epsilon_p(\vec{R}) = \int g^2(z, \vec{R}) [V(\vec{R}, z) - V_{\text{SM}}(\vec{R}, z)] dz .$$

As seen in Table I, it is of order 1% of $|E_0|$ (larger for ${}^3\text{He}$ than for ${}^4\text{He}$ because of its lighter mass).

We next determine the value ϵ_c of the Laplacian term in Eq. (7), using Eq. (A1). This, too, is of order 1%. Collecting these terms the effective potential

for lateral motion is

$$\epsilon(\vec{R}) = E_0 + \Delta\epsilon_p + \epsilon_c , \quad (12)$$

shown in Fig. 1 and Table I.

We have not performed a 2D band-structure calculation with this potential since one already exists.¹⁶ It is possible, however, to use perturbation theory to determine some of the principal features of the lowest band. To that end one needs the Fourier coefficients ϵ_G of the function $\epsilon(\vec{R})$ of Eq. (12). Rather than evaluate the Fourier integrals, we have least-squares fitted coefficients to the Fourier expansion¹⁴

$$\begin{aligned} \epsilon(s_1, s_2) = & \epsilon_0 + 2\epsilon_1 [\cos 2\pi s_1 + \cos 2\pi s_2 + \cos 2\pi(s_1 + s_2)] \\ & + 2\epsilon_2 [\cos 2\pi(s_1 - s_2) + \cos 2\pi(2s_1 + s_2^2) \\ & + \cos 2\pi(s_1 + 2s_2)] . \end{aligned} \quad (13)$$

Here

$$\vec{R} = s_1 \vec{a}_1 + s_2 \vec{a}_2 , \quad (14)$$

where the origin is at the center of the hexagon and \vec{a}_1 and \vec{a}_2 are vectors to the center of neighboring cells. In this notation $(s_1, s_2) = (\frac{1}{2}, 0)$ for the SP point and $(\frac{1}{3}, \frac{1}{3})$ for the A point. The expansion (13) corresponds to including only sets of the two smallest, inequivalent, nonzero reciprocal-lattice vectors \vec{G}_1 and \vec{G}_2 . The values found for the coefficients ϵ_0 , ϵ_1 , and ϵ_2 are -12.19 , -0.33 , and -0.04 meV for ${}^4\text{He}$, and -11.50 , -0.33 , and -0.11 meV for ${}^3\text{He}$, respectively.

We may estimate by perturbation theory various properties of the band structure. The ground-state

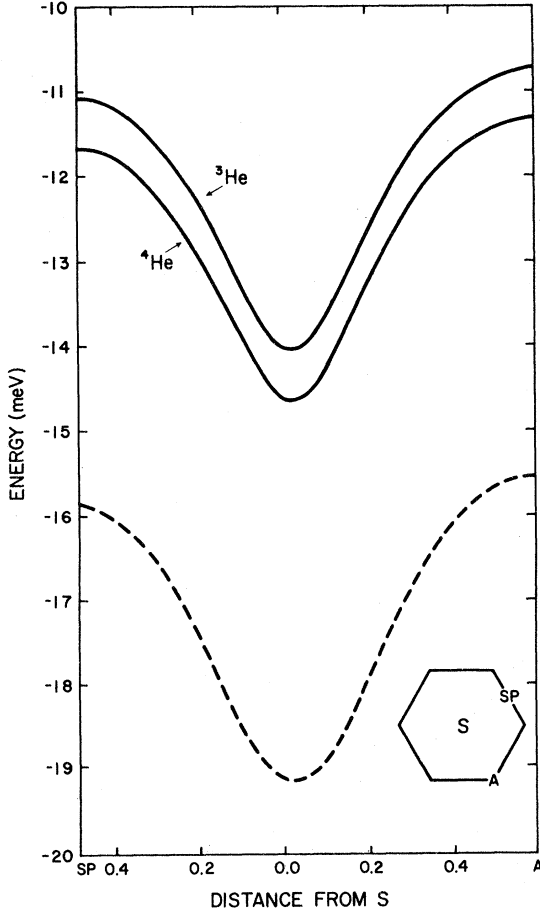


FIG. 1. Dashed curve shows $V_{\min}(\vec{R})$ (defined in the text) for points \vec{R} along symmetry lines $S \rightarrow A$ and $S \rightarrow SP$ in the hexagonal graphite cell (shown in the lower right corner). Full curves show the energy $\epsilon(\vec{R})$ for the two He isotopes in the ground state of motion perpendicular to the surface.

energy (for Bloch state $\vec{K} = 0$) is given by

$$E_0 = \epsilon_0 - 12m\epsilon_1^2/\hbar^2G_1^2,$$

omitting the negligible contributions of G_2 .

The resulting values of $|E_0|$ are 12.33 and 11.69 meV for ^4He and ^3He , respectively. It is necessary to perform one small correction to these before comparing with the previous band-structure calculation. The latter utilized the *experimental* (scattering) eigenvalues of the laterally averaged potential, which are¹² -12.06 ± 0.1 and -11.62 ± 0.1 meV. The eigenvalues of the model potential used in the *present* calculation, however, are¹¹ -12.12 and -11.53 meV. We therefore add the differences ($+0.06$ and -0.09 meV) to our computed values in order to obtain the most realistic values of E_0 . The results are $E_0 = -12.27$ and -11.78 meV for ^4He and ^3He , respectively. We may

now contrast these with the band-structure results³: -12.22 and -11.73 meV (which in turn are in excellent agreement with thermodynamic measurement^{1,2}: -12.27 and -11.72 ± 0.17 meV). The differences are very small, indeed, indicating that the present method is a viable calculational tool. In order to further test this method, we compared the band gaps computed with the 2D potential $\epsilon(\vec{R})$ with those obtained previously.³ We use perturbation theory and neglect coupling to states other than \vec{k} and $\vec{k} + \vec{G}$, which are degenerate in the absence of the ϵ_1 and ϵ_2 terms of Eq. (13). The splitting at the P point (hexagonal corner) in the 2D Brillouin zone is $3|\epsilon_1|$ and at the Q point (midpoint of a hexagon edge) it is $2|\epsilon_1|$. Our methods predicts then 0.99 and 0.66 meV for both isotopes. The more complete and conventional calculation obtained¹⁷ 0.93 (0.86) meV for ^4He (^3He) at the P point and 0.73 (0.64) meV at the Q point. The discrepancies (of order 10%) can probably be attributed to the inadequate incorporation of other states in this perturbation calculation. Thus omitted are higher-lying states of perpendicular motion. To put the interpretation into perspective, note that the principal determinant of the gaps in the conventional method³ is the matrix element of the lowest Fourier component of the potential $V_{\vec{G}}(z)$, between ground-state solutions $\psi(z)$ of the 1D laterally averaged potential ($\langle 0 | V_{\vec{G}} | 0 \rangle$ in the notation of Ref. 3). This has magnitude 0.28 meV according to the measurement of Boato *et al.*¹³ The computed³ band gaps thus have a significant contribution from other states (both on- and off-diagonal).

We address next the probability densities associated with the wave function of Eq. (1). From perturbation theory,¹⁸ the $\vec{K} = 0$ wave function appropriate to Eq. (7) satisfies

$$A_c^{1/2}h_0(\vec{R}) = 1 - \frac{2m}{\hbar^2} \sum'_{\vec{G}} \frac{\epsilon_{\vec{G}}}{G^2} e^{i\vec{G} \cdot \vec{R}} + \left(\frac{2m}{\hbar^2} \right)^2 \sum'_{\vec{G}} \left[\sum'_{\vec{H}} \frac{\epsilon_{\vec{G}} \epsilon_{\vec{H}-\vec{G}} e^{i\vec{H} \cdot \vec{R}}}{G^2 H^2} - \frac{\epsilon_{\vec{G}}^2}{2G^4} \right],$$

normalized to unity in the unit cell, of area $A_c = 5.24 \text{ \AA}^2$. The prime means that the reciprocal-lattice sums exclude zero. The probability density $g_{\vec{G}}^2(z; \vec{R})/\hbar^2$ calculated with this function are shown in Figs. 2 and 3 for ^4He and ^3He . Note the greater localization of the heavier isotope and the tendency of the equal probability contours to follow the variation of $\xi(\vec{R})$, especially near the very repulsive, small z region.

The ^4He density may be used to calculate the mean distance $\langle z \rangle$ above the topmost carbon layer. Our result, $\langle z \rangle = 2.89 \text{ \AA}$, is in very good agreement with the value $\langle z \rangle = 2.85 \text{ \AA}$ obtained recently by Carneiro

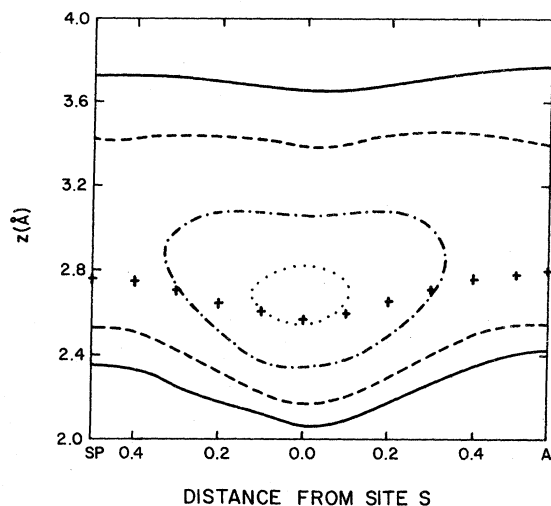


FIG. 2. Contours of equal probability density $\psi^2(z, \bar{R})$ for the ^4He ground-state wave function (normalized over a hexagonal cell). The \bar{R} values lie along the lines $S \rightarrow SP$ and $S \rightarrow A$, respectively (see Fig. 1). Values of ψ^2 (in \AA^{-3}) are 0.6 (dotted curve), 0.25 (dash-dot), 0.05 (dashes), and 0.01 (full curve). The pulses denote the curve $z = \xi(\bar{R})$, the locus of potential minima as a function of z .

*et al.*¹⁹ These workers deduced this from the contribution of a submonolayer ^4He film to the Bragg peak intensity of neutrons scattered by a ^4He -Grafoil system. Comparison can be made with a number of other calculations of $\langle z \rangle$: (a) 2.92 \AA , computed with a wave function $\bar{\psi}(z)$, the solution for the laterally

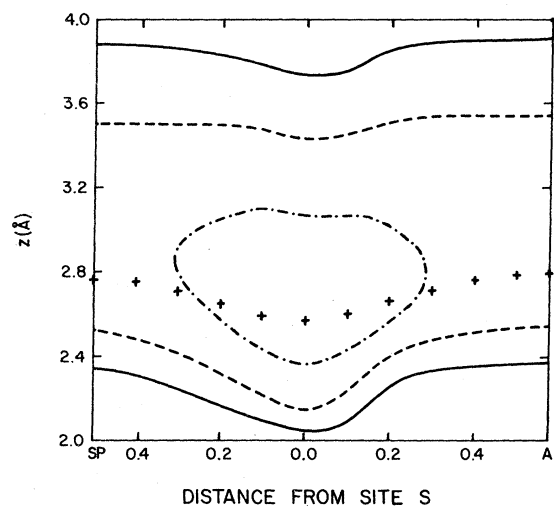


FIG. 3. Same as Fig. 2 for ^3He . There is no region where $\psi^2 \geq 0.6 \text{\AA}^{-3}$.

averaged potential $V_0(z)$, shown in Fig. 4, (b) 2.45 \AA , obtained from the anisotropic Yukawa-6 potential of Ref. 11, and (c) 3.25 \AA , found²⁰ from the venerable isotropic 6-12 potential with parameters chosen prior to the era of scattering experiments. This substantiates further the accuracy of the anisotropic 6-12 potential, which was inspired originally by the scattering data.^{12,13}

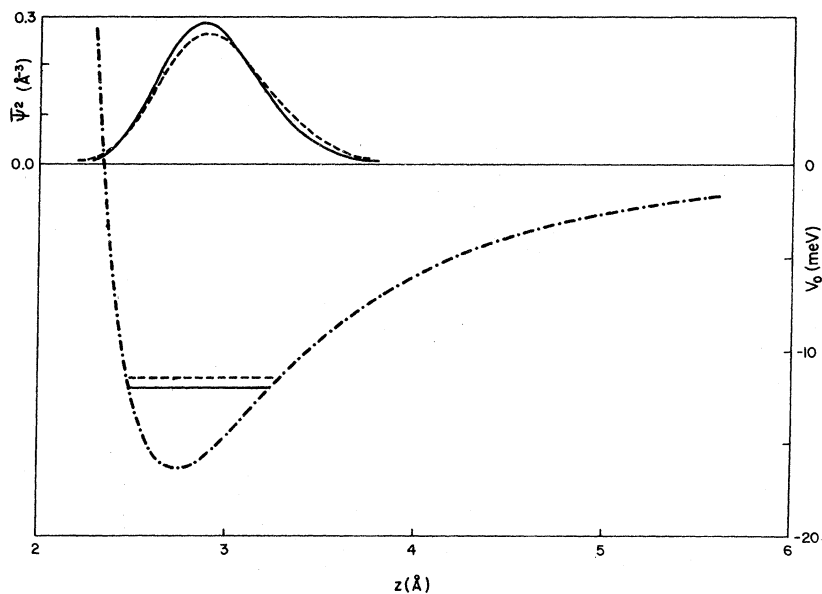


FIG. 4. Laterally averaged potential energy $V_0(z)$ is the dash-dot curve (right ordinate scale). Also shown are the ground-state probability densities and eigenvalues for ^4He (full curve) and ^3He (dashed curve); left ordinate scale.

IV. CONCLUSIONS

We have described a convenient scheme for calculating the spectrum and wave functions of adsorbed quantum gases. The problem is separated into two parts, associated with motion perpendicular and parallel to the surface, respectively. The Schrödinger equation for g can be solved easily by fitting the potential to a shifted-Morse form, Eq. (8). An important feature is that the maximum in g as a function of z follows²¹ the periodic variation of $\xi(\vec{R})$. This minimizes the coupling to excited states perpendicular motion. The numerical example studied finds a very small coupling [which depends on the gradients of both the one-dimensional potential and $\xi(\vec{R})$].

An application is presented in the form of a determination of $\langle z \rangle$ from the probability density $h^2(\vec{R})g^2(z; \vec{R})$. There results a 1% shift from the value calculated using a smooth surface approximation. Agreement with experiment is remarkably good.

$$2m \frac{\epsilon_c(\vec{R})}{\hbar^2} = \frac{(b-1)}{4} \left[\frac{2b^2-1}{b(b-1)^2} - \frac{(b-1)}{(b-2)^2} + f^2 + \zeta(2, b-1) \right] \left[\frac{\vec{\nabla} \alpha}{\alpha} \right]^2 - \frac{1}{4} \left[b-1 + \left(\frac{b}{b-2} \right)^2 - b^2 \zeta(2, b-1) \right] \times \left[\frac{\nabla b}{b} \right]^2 + \frac{b-1}{4} (\alpha \vec{\nabla} \xi)^2 - \left[f - \frac{2b}{b-1} + \frac{b(b-1)}{(b-2)^2} \right] \frac{\vec{\nabla} \alpha \cdot \vec{\nabla} b}{2\alpha b} + \frac{(b-1)f}{2} \frac{\vec{\nabla} \alpha \cdot \vec{\nabla} \xi}{\alpha} - \frac{\alpha}{2b} \vec{\nabla} b \cdot \vec{\nabla} \xi ,$$

(A1)

$$f \equiv \psi(b) - \ln b .$$

(A2)

Here $\zeta(2, b-1)$ is the Riemann zeta function and $\psi(b)$ is the digamma function.

ACKNOWLEDGMENTS

We are indebted to G. Whitfield, P. B. Shaw, J. D. Maynard, W. A. Steele, D. R. Frankl, and S. R. Polo for helpful and stimulating discussions. This research was supported in part by U.S. DOE Contract No. DE-AS02-79ER10454 and by a travel grant from CNR through GNSM-Unità Basse Temperature, Padova, Italy.

APPENDIX

We compute here the term ϵ_c defined in Eq. (6), using the definition of Eq. (5b). The calculation can be accomplished accurately with the shifted-Morse potential and wave functions of Sec. II. After some lengthy algebra, we obtain the following result:

*Permanent address: Instituto di Fisica, Università di Padova, Padova, Italy.

¹R. L. Elgin and D. L. Goodstein, Phys. Rev. A 9, 2657 (1974).

²R. L. Elgin, J. M. Greif, and D. L. Goodstein, Phys. Rev. Lett. 41, 1723 (1978).

³W. E. Carlos and M. W. Cole, Phys. Rev. B 21, 3713 (1980).

⁴H.-W. Lai, C.-W. Woo, and F. Y. Wu, J. Low Temp. Phys. 3, 463 (1970).

⁵C. E. Harvie and J. H. Weare, Phys. Rev. Lett. 40, 187 (1978); N. Garcia, V. Celli, and F. O. Goodman, Phys. Rev. B 19, 1808 (1979).

⁶C. Schwartz, M. W. Cole, and J. Pliva, Surf. Sci. 75, 1 (1978).

⁷F. O. Goodman, N. Garcia, and V. Celli, Surf. Sci. 85, 317 (1979).

⁸M. W. Cole and T. T. Tsong, Surf. Sci. 69, 325 (1977); E. Ghio, L. Matterna, C. Solvo, F. Tommasini, and U. Valbusa, J. Chem. Phys. (in press).

⁹We note in passing that the very large anharmonic form of typical potentials precludes use of a parabolic potential except for quite massive (i.e., localized) particles.

¹⁰L. Infeld and T. E. Hull, Rev. Mod. Phys. 23, 21 (1951).

In Sec. III we treat the deviation of the potential from the shifted-Morse form.

¹¹W. E. Carlos and M. W. Cole, Surf. Sci. 91, 339 (1980).

¹²G. Derry, D. Wesner, W. E. Carlos, and D. R. Frankl, Surf. Sci. 87, 629 (1979).

¹³G. Boato, P. Cantini, C. Guidi, R. Tatarek, and G. P. Felcher, Phys. Rev. B 20, 3957 (1980).

¹⁴W. A. Steele, Surf. Sci. 36, 317 (1973).

¹⁵As noted in Ref. 4, one excludes the region of unphysical divergent behavior of $V_{6-12}(\vec{r})$.

¹⁶More precisely, Ref. 3 presents an empirical band-structure calculation using the same bound-state resonances and matrix elements (Refs. 12 and 13) used to determine this potential (Ref. 11).

¹⁷See Table I of Ref. 3.

¹⁸L. D. Lanđau and E. M. Lifshitz, *Quantum Mechanics* (Perigamon, London, 1959).

¹⁹K. Carneiro, L. Passell, W. Thomlinson, and H. Taub (unpublished).

²⁰A. D. Novaco, Phys. Rev. B 13, 3194 (1976).

²¹The maximum in probability density for the wave function of Eq. (10a) is at $z = \xi - \alpha^{-1} \ln(1 - b^{-1})$. The second term is of order 0.15 Å here.